
A Study of the Numerical Stability of the Method of Contour Dynamics

G. R. Baker

Phil. Trans. R. Soc. Lond. A 1990 **333**, 391-400

doi: 10.1098/rsta.1990.0167

Email alerting service

Receive free email alerts when new articles cite this article - sign up in the box at the top right-hand corner of the article or click [here](#)

To subscribe to *Phil. Trans. R. Soc. Lond. A* go to:

<http://rsta.royalsocietypublishing.org/subscriptions>

A study of the numerical stability of the method of contour dynamics

BY G. R. BAKER

Department of Mathematics, Ohio State University, Columbus, Ohio 43210, U.S.A.

The inviscid interaction of vortex structures has been studied extensively to elucidate many of the important features of high Reynolds number flows and turbulence. Contour dynamics was developed specifically to study the evolution of the boundaries of uniform vortices, and has been used to study a wide variety of flows. The method is a lagrangian one, and typically a discrete dynamical system is obtained by representing the boundary by a finite collection of points. We examine the linear stability features of a typical method by considering perturbations to a circular, uniform vortex. We find a spurious branch to the numerical dispersion relation that indicates points will oscillate along the boundary without any distortion in its shape. Numerical results for the full equations show that the amplitudes of these particular modes grow slowly in time.

1. Introduction

A compelling motivation for the study of vorticity is the observation of organized structures in turbulent flows. For example, in turbulent shear layers a thin layer of vorticity rolls up into roughly elliptical structures that subsequently undergo merger or annihilation during strong interaction with nearest neighbours. While most of the vorticity points transversely to the flow, there are also thin filaments lying mostly in the plane of the flow along the braids connecting the larger vortices, but becoming entangled in the larger vortices. In turbulent boundary layers, hairpin vortices rise up out of the boundary layer. Numerical simulations of homogeneous turbulence show tangled vortex filaments. Consequently, it is tempting to model the global features of turbulent flow by studying the inviscid interaction of vortex structures in the belief that viscous effects have only a slow effect on vortex structures. However, it is not clear what choice for the vorticity distribution in each structure is best, and so a great simplification is made by considering only simple distributions in the hope that the global properties of the vortices and their interactions are not sensitively dependent on the fine details of the vorticity distribution. See Saffman & Baker (1979) for a fuller discussion of the role of vorticity and for the definition of the terminology that we will use in this paper.

For inviscid flow of a fluid with constant density, the equations of motion may be written as a transport equation for the vorticity ω ;

$$\partial\omega/\partial t + \mathbf{u} \cdot \nabla\omega = \omega \cdot \nabla\mathbf{u}. \quad (1)$$

The vorticity is advected with the fluid velocity \mathbf{u} , which may be determined as a functional of the vorticity through the relations,

$$\nabla \times \mathbf{u} = \omega, \quad \nabla \cdot \mathbf{u} = 0. \quad (2)$$

Phil. Trans. R. Soc. Lond. A (1990) **333**, 391–400

Printed in Great Britain

391

Equation (1) is not strictly hyperbolic in that the velocity depends globally on the vorticity through equation (2), but it is possible to write the equation in conservation form,

$$\frac{D}{Dt} \int_V \omega dV = 0, \quad (3)$$

where the integration is over a vortex tube, and the time derivative is with the flow of the fluid. Equation (3) presents an obvious way that lagrangian methods may be used to study fluid flow.

To be effective in the study of turbulence or flows at high Reynolds number, vorticity distributions must be chosen that capture the form of those observed naturally or in experiments. The simplest model for a vortex filament is a curved vortex line. Unfortunately, a curved vortex line is not a dynamically consistent idealization, but it is difficult to find alternate distributions whose form permits a tractable study by analysis or computation. A great simplification is afforded if the flow depends on only two spatial coordinates. In particular, vorticity in two-dimensional flow is a scalar which advects with the flow; the stretching term $\omega \cdot \nabla \mathbf{u} = 0$. In two-dimensional flow, a vortex line becomes a vortex point. Although not strictly a weak solution for the Euler equations (Turkington 1987), point vortices provide the simplest model for vortex interaction. A more realistic model of a vortex in flow at high Reynolds number is the uniform vortex, representing a vortex of finite area. A uniform vortex is a region of uniform vorticity enclosed by a boundary. The notion of a uniform vortex may be generalized to flows that depend on only two coordinates in a curvilinear coordinate system, and where the vorticity points out of the surface which contains the flow. We shall call this generalization a vortex patch. Note that the vorticity distribution is no longer uniform in general for vortex patches. An example is given in the study of the motion of vortex rings by Pozrikidis (1986). In this paper we will concentrate on the dynamics of uniform vortices, that is, vortex patches in two-dimensional flow.

2. The equations of motion

One advantage to the choice of a uniform vortex as a model for a vortex structure in high Reynolds number flow is that it is a weak solution to Euler's equations, and that its motion is described by the evolution of its boundary. According to the theory of Yudovich (1963), a uniform vortex exists globally in time. While the fluid velocity away from the boundary remains smooth for all time, the theory does not exclude the possibility of the boundary forming curvature singularities in finite time.

An evolution equation for the boundary of a uniform vortex is derived usually from the Biot–Savart integral that gives \mathbf{u} in terms of ω as a formal solution to (2). Specifically in two-dimensional flow, the vorticity points out of the plane, $\omega = \omega \mathbf{k}$, \mathbf{k} a unit vector and ω a constant inside the boundary, and the velocity $\mathbf{u}(x, y) = (u(x, y), v(x, y))$ is given by

$$\begin{aligned} u(x, y) &= \omega \int_A \frac{\partial}{\partial y'} G(|\mathbf{x} - \mathbf{x}'|) dx' dy', \\ v(x, y) &= -\omega \int_A \frac{\partial}{\partial x'} G(|\mathbf{x} - \mathbf{x}'|) dx' dy'. \end{aligned} \quad (4)$$

Here $G(|\mathbf{x} - \mathbf{x}'|) = (1/2\pi) \ln |\mathbf{x} - \mathbf{x}'|$ is the free space Greens function for Laplace's equation in two-dimensions. By use of Greens theorem,

$$\begin{aligned} u(x, y) &= -\omega \int G(|\mathbf{x} - \mathbf{x}(q)|) \frac{dx}{dq} dq, \\ v(x, y) &= -\omega \int G(|\mathbf{x} - \mathbf{x}(q)|) \frac{dy}{dq} dq. \end{aligned} \quad (5)$$

The integration is now along the boundary of the patch $(x(q), y(q))$. Actually, both the velocity and the boundary depend on time, but for convenience the implicit dependency on time is not shown. The evolution of the boundary follows from (3) and is given by

$$\begin{aligned} \frac{dx}{dt}(p) &= -\frac{\omega}{4\pi} \int \ln [(x(p) - x(q))^2 + (y(p) - y(q))^2] \frac{dx}{dq} dq, \\ \frac{dy}{dt}(p) &= -\frac{\omega}{4\pi} \int \ln [(x(p) - x(q))^2 + (y(p) - y(q))^2] \frac{dy}{dq} dq. \end{aligned} \quad (6)$$

Zabusky *et al.* (1979) were the first to use this form to develop a lagrangian numerical method to study the evolution of uniform vortices. Their approach has been followed by others, notably Dritschel (1988) and Pozrikidis & Higdon (1985). Other researchers (see, for example, Pullin & Jacobs 1986; Broadbent & Moore 1985; Baker & Shelley 1990) prefer to use an alternate form, obtained by executing an integration by parts,

$$\begin{aligned} \frac{dx}{dt}(p) &= \frac{\omega}{2\pi} \int \frac{x(p) - x(q)}{R} \left\{ (x(p) - x(q)) \frac{dx}{dq} + (y(p) - y(q)) \right\} \frac{dy}{dq} dq, \\ \frac{dy}{dt}(p) &= \frac{\omega}{2\pi} \int \frac{y(p) - y(q)}{R} \left\{ (x(p) - x(q)) \frac{dx}{dq} + (y(p) - y(q)) \right\} \frac{dy}{dq} dq, \end{aligned} \quad (7)$$

where $R = (x(p) - x(q))^2 + (y(p) - y(q))^2$. The main difference between (6) and (7) is that in one case the integrand contains an integrable singularity, whereas in the other the integrand has a removable singularity. Equation (7) can be cast into a compact form by the introduction of complex variables. Let $z(p) = x(p) + iy(p)$, then

$$\frac{dz^*}{dt}(p) = -\frac{\omega}{4\pi} \int \frac{z^*(p) - z^*(q)}{z(p) - z(q)} \frac{dz}{dq} dq, \quad (8)$$

where the star superscripts refer to taking the complex conjugate. Similarly, (6) may be written in complex form;

$$\frac{dz^*}{dt}(p) = \frac{\omega}{4\pi} \int \ln (z(p) - z(q)) \frac{dz^*}{dq} dq. \quad (9)$$

In general, (6) or (7) are solved numerically by the method of lines. The boundary is represented by a finite collection of points, z_j , $1 \leq j \leq N$, and the integrals that determine the evolution of z_j are replaced by finite sums over all the points. However, the integrands depend on derivatives which must be approximated also. The result is that the evolution equations for z_j form a large system of ordinary differential equations that may be solved by standard methods, such as Runge-Kutta or

predictor–corrector methods. The overall accuracy will depend on the spatial accuracy of the numerical quadrature and the temporal accuracy of the method used to advance the solution in time. Because the integrands are periodic if the boundary is closed or extends to infinity periodically, the trapezoidal rule may be used with spectral accuracy on the integrands in equation (7). Unfortunately, when separate regions of the boundary approach one another, the integrand is nearly singular and it requires extra effort to maintain spectral accuracy (Baker & Shelley 1990). Alternatively, the boundary may be broken up into little segments that are approximated well by low-order polynomial expressions, but the integrals must still be integrated numerically in each interval, except for simple cases (Pullin 1981; Dritschel 1988). As a specific example of a numerical method, consider the trapezoidal approximation to equation (8):

$$\frac{dz_j^*}{dt} = \frac{\omega h}{4\pi} \sum_{p \neq j} \left\{ \frac{z_j^* - z_p^*}{z_j - z_p} (Dz)_p \right\} + \frac{\omega h}{4\pi} (Dz)_j, \quad (10)$$

where $(Dz)_j$ stands for some approximation to the derivative of $z(p)$ evaluated at z_j .

Presently, there is no rigorous justification for these methods, but they have been applied without apparent difficulty to several flow problems. Since most researchers carry out careful resolution studies, there is little doubt that these methods work well in general. Surprisingly though, few researchers report on the results of an analysis of the linear stability for their methods even though there are some cases where the analysis can be completed. Since there is much interest currently in the formation of small-scales structures that may lead to effects such as filamentation and possible curvature singularities, it is important to understand the accuracy and stability of the numerical methods as far as possible. The purpose of this paper is to shed some light on the stability of a typical method, such as equation (10).

3. Numerical stability

The full nonlinear stability of these methods has not yet been studied, and even a general linear stability analysis is hard because it will depend on the motion of the boundary. However, there are two well-known stationary solutions to (8) or (9), corresponding to a circular vortex and a uniform layer of finite thickness. The stability of these solutions are also well-known; Kelvin (1880) showed that a small perturbation to the circular vortex may be written as the linear superposition of sinusoidal modes. His analysis was done using Euler's equations for fluid flow. We will use the circular vortex as the stationary solution on which we may perform a linear stability analysis of the numerical method, described by equation (10).

The circular vortex is not a stationary solution to the lagrangian equations (see (8)) since points on the boundary rotate along the perimeter with speed $\frac{1}{2}\omega a$, where a is the radius. In general, stationary uniform vortices are found from the requirement that the normal component of the fluid velocity vanishes along the boundary;

$$\mathcal{T} \left\{ \frac{dz}{dp} \frac{dz^*}{dt} \right\} = 0.$$

The tangential component will vary along the boundary. In fact, the tangential motion of the lagrangian points frequently complicates efficient numerical solution of the motion of the boundary. The remedy involves either changing the definition

of the tangential speed (Baker & Shelley 1990) or redistributing points (Dritschel 1988). For purposes of conducting a linear stability analysis, we add a rotational velocity so that the lagrangian points are frozen on the boundary. Thus we consider

$$\frac{dz^*}{dt} = \frac{1}{2}i\omega z^* + \frac{\omega}{4\pi} \int \frac{z^*(p) - z^*(q)}{z(p) - z(q)} \frac{dz}{dq} dq \quad (11)$$

and now $z(p) = ae^{ip}$, $0 \leq p \leq 2\pi$ is a stationary solution, describing a circular vortex with radius a . Consider a small perturbation of the form $z(p) = a \exp(ip)(1 + \epsilon g(p))$. By substituting into (11) and retaining terms up to order ϵ , we obtain the linearized equation,

$$\frac{dg^*}{dt} = \frac{1}{2}i\omega g^* - \frac{i\omega}{4\pi} \int g(q) dq + \frac{i\omega}{4\pi} \int \frac{e^{iq} g^*(p) - e^{ip} g^*(q) + e^{ip} g(p) - e^{iq} g(q)}{e^{ip} - e^{iq}} dq \quad (12)$$

We follow Kelvin (1880) by assuming

$$g(p) = \alpha(t) e^{ikp} + \beta(t) e^{-ikp}, \quad (13)$$

with $k = 1, 2, 3, \dots$. A general perturbation is made up by a linear superposition with various k . The integrals in (12) may be performed by the use of complex integration around a unit circle. By balancing coefficients for each Fourier mode, we obtain the following system

$$d\alpha/dt = 0, \quad d\beta^*/dt = \frac{1}{2}i\omega(\beta^* + \alpha). \quad (14)$$

This system has two linearly independent solutions; thus there are two uncoupled solutions for the motion of the perturbation. One gives the well-known result

$$z(p) = a e^{ip}(1 + \epsilon C e^{i(kp - \frac{1}{2}\omega t)}), \quad (15)$$

where C is some complex constant, but the other solution,

$$\begin{aligned} z(p) &= a e^{ip}(1 + i\epsilon C_1 \sin(kp) + i\epsilon C_2 \cos(kp)) \\ &\approx a \exp [i(p + i\epsilon C_1 \sin(kp) + i\epsilon C_2 \cos(kp))], \end{aligned} \quad (16)$$

arises entirely from the use of a lagrangian approach. It portrays the fact that there are many possible parametrizations for the circle. Thus one may perturb the positions of the lagrangian points along the boundary without change of shape and still maintain a stationary solution. Obviously, the result in (16) is not dynamically important, but it does illustrate that some care must be used in interpreting stability results based on a lagrangian formulation of the equations.

We turn now to the linear stability of the discrete system, equation (10). First, we must specify our approximation, $(Dz)_j$. We take the simplest choice to illustrate the nature of the stability analysis.

$$(Dz)_j = (z_{j+1} - z_{j-1})/2h. \quad (17)$$

The obvious choice for the lagrangian points is $z_j = a e^{ijh}$, $j = 0, 1, 2, \dots, N-1$ where $h = 2\pi/N$, but these points will not be stationary; they will move along the boundary with a constant tangential speed. So, we add a rotational velocity to make the points on the boundary stationary just as we did in (11). Thus we consider

$$\frac{dz_j^*}{dt} = \frac{1}{2}i\omega z_j^* + \frac{\omega h}{4\pi} \sum_{\substack{p=0 \\ p \neq j}}^{N-1} \left\{ \frac{z_j^* - z_p^*}{z_j - z_p} (Dz)_p \right\} + \frac{\omega h}{4\pi} (Dz)_j \quad (18)$$

where $\hat{\omega} = (\omega/h) \sin h$. Now consider a small perturbation of the form, $z_j = a \exp(ijh)(1 + \epsilon g_j)$. By substituting into (18) and retaining only terms up to order ϵ , we obtain

$$\frac{dg_j^*}{dt} = \frac{i\hat{\omega}}{2} g_j^* + \frac{\omega}{8\pi} \left[g_{j+1}^* e^{-ih} - g_{j-1}^* e^{ih} - \sum_{\substack{p=0 \\ p \neq j}}^{N-1} (g_{p+1} e^{ih} - g_{p-1} e^{-ih}) \right] \\ + \frac{i\omega}{4\pi} \sin(h) \sum_{\substack{p=0 \\ p \neq j}}^{N-1} \frac{g_p^* e^{iph} - g_p^* e^{ijh} + g_j e^{ijh} - g_p e^{iph}}{e^{ijh} - e^{iph}}. \quad (19)$$

A general perturbation may be constructed from a linear combination of factors of the form, $g_j = \alpha e^{ijkh} + \beta e^{-ijkh}$, with $k = 1, 2, \dots, \frac{1}{2}N - 1$. We have taken N as even. The case $k = \frac{1}{2}N$ will be considered separately. By balancing terms with $\exp(\pm ijkh)$, we obtain

$$\frac{d\alpha}{dt} = -\frac{1}{2}i\hat{\omega} \alpha + \frac{i\omega}{4\pi} [\beta^* \sin((k-1)h) + \beta^* \sin(h) \phi(k) \\ + \alpha \sin((k+1)h) - \alpha \sin(h) \phi^*(-k)], \\ \frac{d\beta^*}{dt} = \frac{1}{2}i\hat{\omega} \beta^* + \frac{i\omega}{4\pi} [\alpha \sin((k+1)h) - \alpha \sin(h) \phi^*(-k) \\ + \beta^* \sin((k-1)h) + \beta^* \sin(h) \phi(k)], \quad (20)$$

where

$$\phi(k) = \sum_{\substack{p \neq j \\ p=0}}^{N-1} \frac{e^{i(p-j)h} - e^{i(p-j)kh}}{1 - e^{i(p-j)h}}. \quad (21)$$

Despite appearances, $\phi(k)$ does not depend on j . In the appendix, we show how this sum may be evaluated. The result is

$$\phi(k) = \begin{cases} 1-k & \text{for } 1 \leq k \leq \frac{1}{2}N, \\ 1-k-N & \text{for } -\frac{1}{2}N \leq k \leq 1. \end{cases} \quad (22)$$

Finally, we obtain the following system for the coefficients.

$$\frac{d\alpha}{dt} = -\frac{1}{2}i\omega [F(k) \alpha + G(k) \beta^*], \\ \frac{d\beta^*}{dt} = (i\omega \sin(h)/2h) (\beta^* + \alpha) - \frac{1}{2}i\omega [F(k) \alpha + G(k) \beta^*], \quad (23)$$

where

$$F(k) = (1/2\pi) ((k+1) \sin(h) - \sin((k+1)h)) \\ G(k) = (1/2\pi) (k-1) \sin(h) - \sin((k-1)h). \quad (24)$$

A general solution has the form $\alpha = A e^{\frac{1}{2}i\omega t}$, $\beta^* = B e^{\frac{1}{2}i\omega t}$, where

$$\sigma^2 + (G(k) + F(k) - h^{-1} \sin(h)) \sigma + (G(k) - F(k)) h^{-1} \sin(h) = 0. \quad (25)$$

Note that as $h \rightarrow 0$, $F(k) \rightarrow 0$ and $G(k) \rightarrow 0$, and this equation then has roots $\sigma = 0, 1$, which agrees with the results in (15) and (16). Since $F(k) \geq G(k)$ for $1 \leq k < \frac{1}{2}N$, σ has real roots.

Now we consider the case, $k = \frac{1}{2}N$. We write $g_j = \beta(-1)^j$ and substitute into (19). We obtain

$$\frac{d\beta^*}{dt} = i\omega \sin(h) \left(\left(\frac{1}{4h} + \frac{1}{2\pi} \right) \beta^* + \left(\frac{1}{4h} - \frac{1}{2\pi} \right) \beta \right). \quad (26)$$

Contour dynamics

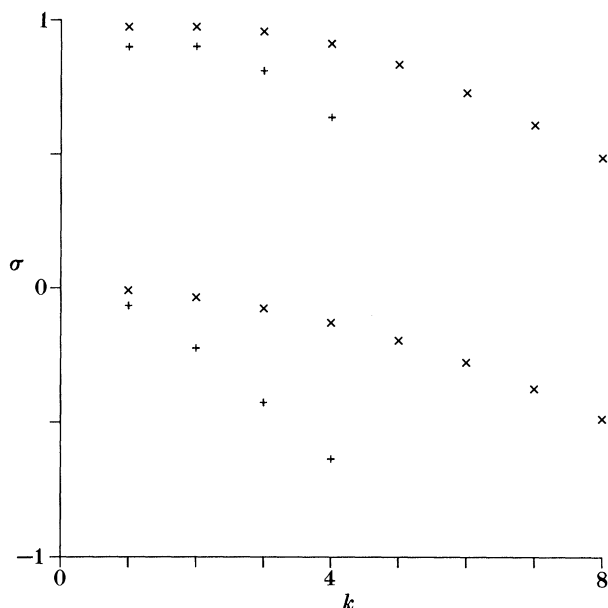


Figure 1. The values of σ for various k when $N = 8$ (+) and $N = 16$ (x).

The general solution to this equation is $\beta^* = A e^{\frac{1}{2}i\omega t} + B e^{-\frac{1}{2}i\omega t}$ where $\sigma = (2/\pi h)^{\frac{1}{2}} \sin(h)$. Rather than two propagating modes, there is a single standing mode.

Since none of the solutions to the perturbation equation (19) grow in time, we have shown that the numerical method is linearly stable, assuming of course that a sufficiently small timestep is used in the method to advance the discrete system in time. The choice for the approximation to the derivative, equation (17), is not crucial. For instance, if the discrete fourier series that is obtained by collocation with the discrete points is differentiated, then the results above hold with the expression $\sin(f(k)h)$ replaced by $f(k)h$. In this case, the physically correct value for σ is obtained, except for the case $k = \frac{1}{2}N$. For other approximations to the derivative, different functions of k will replace the expression $\sin(f(k)h)$ but they should lie between $\sin(f(k)h)$ and $f(k)h$.

In figure 1, we display the values of σ for two cases, $N = 8$ and $N = 16$. Note that the better the resolution the better the agreement with the physically correct values, the agreement being best for the lower values of k . Even so, the finite values of σ on the lower branch, that should be zero, indicate that perturbations in the positions of the discrete lagrangian points will lead to spurious oscillatory behaviour.

These results raise new questions. Since there are two distinct branches describing a discrete dispersion relation, it is possible for near resonances to occur that may drive spurious nonlinear instabilities. What happens to the spurious oscillations for finite amplitudes? The latter question may be addressed by direct numerical computation. The discrete system, equation (18), with equation (17), was advanced in time by a fourth-order Adams–Moulton predictor–corrector. Starting values were obtained by a fourth-order Runge–Kutta. The initial condition was taken to be

$$z_j = a \exp [i(jh + \epsilon \sin(jkh))]. \quad (27)$$

Obviously, the true physical behaviour is for the points to remain stationary. For the results reported below, $\epsilon = 0.1$, $a = \omega = 1$.

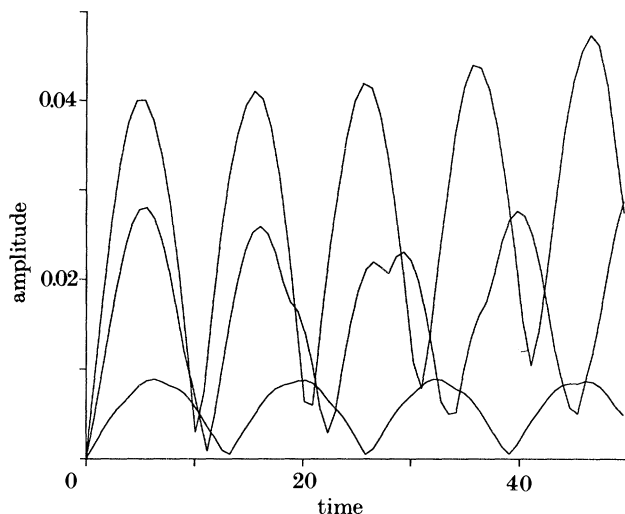


Figure 2. The temporal variation of A for $k = 1, 2, 3$. The larger the value of k , the higher the peak in A .

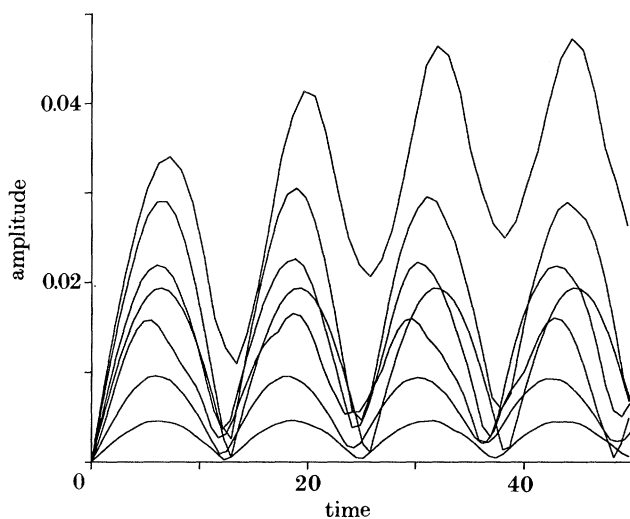


Figure 3. The temporal variation of A for $k = 1, 2, 3, 4, 5, 6, 7$. The larger the value of k , the higher the peak in A .

As the points oscillate, they move off the circle. We measure their deviation from the circular boundary by

$$A = \frac{1}{N} \sum_{j=0}^{N-1} ||z_j| - 1|. \quad (28)$$

Viewed in the eulerian frame, A measures the amplitude of an oscillation about the circular boundary. In figure 2, we show how A varies in times for the modes $k = 1, 2, 3$ when $N = 8$. Despite the fact that the perturbation shifts points along the boundary only, both linear modes described by (25) are excited, leading to the appearance of a modulated oscillation. Contrary to linear theory however, the

modulated oscillations grow slowly in time. In figure 3, we show the temporal variation of A for the modes $k = 1, 2, 3, 4, 5, 6, 7$ when $N = 16$. Observe that for $k = 1, 2, 3$ the amplitudes are less than the corresponding ones for $N = 8$. With higher resolution, these oscillations depart less from the stationary boundary. Furthermore (ignoring the mode $k = 8$), the highest mode $k = 7$ for $N = 16$ does not have a significantly higher amplitude than the highest mode $k = 3$ for $N = 8$.

We conclude that, although there is evidence of a weak instability for a typical numerical method applied to the evolution of the boundaries of uniform vortices, the numerical method is reliable since the indications are that the growth rate is bounded and decreases with improved resolution. Generally, the motion of the boundary will be on a faster scale than these slowly growing oscillations, so our analysis may not be relevant. Nevertheless, we recommend that numerical results be checked carefully for possible contamination by spurious oscillations in the tangential directions.

This work has been partly supported by the National Science Foundation under Grant DMS-8352067. I am also very grateful to Professor D. W. Moore of Imperial College, London, for suggesting this problem, and for many stimulating discussions.

Appendix

Here we determine the value of the sum, $\phi(k)$. First, we rewrite the sum by shifting the summation variable and by using the periodicity of the summand.

$$\phi(k) = \sum_{p=1}^{N-1} \frac{e^{iph} - e^{ipkh}}{1 - e^{iph}}. \quad (\text{A } 1)$$

Consider the integral in the complex plane,

$$I(k) = \frac{1}{2\pi i} \int_{|z|=R} \frac{z^{k-1}}{(1-z)(z^N-1)} dz \quad (\text{A } 2)$$

with $1 \leq k \leq \frac{1}{2}N$. For large R , $I \rightarrow 0$. The integrand has first-order poles at e^{iph} , $p = 1, 2, \dots, N-1$ with residue

$$e^{ipkh}/N(1 - e^{iph}),$$

and a second order pole at 1 with residue

$$(1/2N)(N+1-2k)$$

Thus we obtain the result,

$$\sum_{p=1}^{N-1} \frac{e^{ipkh}}{1 - e^{iph}} = k - \frac{1}{2} - \frac{1}{2}N, \quad (\text{A } 3)$$

which may be used to evaluate $\phi(k)$ directly for $1 \leq k \leq \frac{1}{2}N$. When $-\frac{1}{2}N \leq k \leq 1$, the integrand in (A 1) has another pole at the origin with residue -1 . Consequently, we are lead to the results expressed in (22).

References

- Baker, G. R. & Shelley, M. J. 1990 *J. Fluid Mech.* (In the press.)
 Broadbent, E. G. & Moore, D. W. 1985 *Phys. Fluids* **28**, 1561.
 Dritschel, D. 1988 *J. Comput. Phys.* **77**, 240.
Phil. Trans. R. Soc. Lond. A (1990)

- Lord Kelvin (Thompson, W.) 1880 *Phil. Mag.* **X**, 155.
- Pozrikidis, C. 1986 *J. Fluid Mech.* **168**, 337.
- Pozrikidis, C. & Higdon, J. J. L. 1985 *J. Fluid Mech.* **157**, 225.
- Pullin, D. I. & Jacobs, P. A. 1986 *J. Fluid Mech.* **171**, 377.
- Saffman, P. G. & Baker, G. R. 1979 *A. Rev. Fluid Mech.* **11**, 95.
- Turkington, B. 1987 *Arch. Ration. Mech. Anal.* **97**, 75.
- Yudovich, V. I. 1963 *Zh. Vych. Mater.* **3**, 1032.
- Zabusky, M. J., Hughes, M. H. & Roberts, K. U. 1979 *J. Comput. Phys.* **30**, 96.